Damage of Infill Masonry Walls due to Vertical Loads in Buildings with Reinforced Concrete Structure

JOSÉ MIRANDA DIAS
Department of Buildings,
National Laboratory of Civil Engineering (LNEC),
Av. do Brasil 101, Lisbon,
PORTUGAL

Abstract: Buildings are subjected to deformations of their reinforced concrete structure due to vertical loads that can lead, in certain cases, to the significant cracking of the unreinforced masonry (URM) infill walls, therefore requiring the development of specific knowledge of these types of deformations in order to minimise them.
Aiming the evaluation of buildings with reinforced concrete structures subjected to vertical deformations, the mechanical characteristics of their infill masonry walls, as well as of their interface with the supporting concrete elements, are here analysed. The basic compression behaviour of brick masonry is assessed particularly through the previous analysis of a vertical compression test of a masonry specimen. The mechanical behaviour characteristics of the constituents (bricks, and mortar joints) are analysed to account for their influence on the compression behaviour of masonry infill, aiming particularly for the prevision of their cracking in case of vertical deformations of the supporting reinforced concrete (RC) elements. Based on that evaluation, the analysis of masonry walls subjected to vertical deformations of their supports is made through the assessment of the relevant characteristic behaviour of masonry wall-beam/slab assembly in case of vertical load. A general modelling approach of the behaviour of URM infills and the interaction with their supports is generally accessed. F inally, the preventive control of deformations of masonry wall-beam/slab assembly is discussed.

Key-Words: Masonry infill walls; Reinforced concrete elements; Vertical loads; Buildings

Received: January 14, 2023. Revised: March 16, 2023. Accepted: March 30, 2023. Published: April 4, 2023.

1 Introduction

Buildings are subjected to deformations of their reinforced concrete structure due to vertical loads that can lead, in certain cases, to the significant cracking of the unreinforced masonry (URM) infill walls, therefore requiring the development of specific knowledge of these types of deformations in order to minimise them.
Aiming the evaluation of buildings with reinforced concrete structures subjected to vertical deformations, the mechanical characteristics of their URM infill walls, as well as of their interface with the supporting concrete elements, are here analysed, in view of a possible further development of that evaluation specifically using numerical analysis in the respective study. The basic compression behaviour of brick masonry is assessed particularly through the analysis of a vertical compression test of a masonry specimen.

The mechanical behaviour characteristics of the constituents (bricks, and mortar joints) are analysed in order to account for their influence on the compression behaviour of masonry infill, aiming particularly for the prevision of their cracking in case vertical deformations of the supporting reinforced concrete (RC) elements. Based on that evaluation, the analysis of masonry walls subjected to vertical deformations of their supports is made through the assessment of the relevant characteristic behaviour of masonry wall-beam/slab assembly in case of vertical load. A general modelling approach of the behaviour of URM infills and the interaction with their supports is generally accessed. Finally, the preventive control of deformations of masonry wall-beam/slab assembly is discussed.

2 Challenges in the Study of URM Infills Cracking due to Vertical Deflections and Methodology of the Study

Masonry is a composite material made of units (bricks or blocks) linked through joints (with or without mortar), and these units exhibit a large range of geometry and elastic / inelastic properties. The orthotropic behaviour of masonry, in terms of the dependence of elastic response on the orientation, is particularly related to their geometrical arrangement, as well as to the different elastic mechanical properties of unit and mortar joints. These characteristics, together with a diversity of possible arrangement of units and mortar characteristics, can particularly lead to a relatively wide variation of the masonry mechanical behaviour and the correspondent failure mechanisms, although some general features can be found, especially in terms of their overall mechanical behaviour.

Vertical deflections of the structural supporting elements of URM infills (beams or slabs of reinforced concrete), can be sufficiently high to transmit loads to these masonry walls, especially in certain conditions of low rigidity of these supporting elements. These excessively high vertical deflections of the supporting reinforced concrete (RC) elements (slabs/beams) of the URM infills can be especially associated with creep effects, which in certain cases can produce long-term deflections of these RC elements significantly greater than the correspondent deflections after construction. Creep effects in RC elements depend on diverse factors, such as the ambient humidity, the dimensions of the element, the composition of the concrete, and the duration and magnitude of the loading (see Eurocode 2: EN 1992-1-1:2004, 3.1.4, (1)P, [5]).

The excessive vertical deformations of the RC elements can eventually lead to the URM infills cracking, due to their brittle characteristics and their limited resistance to tension, compression, and shear actions, particularly in the mortar joints, which require the adequate assessment of the respective mechanical characteristics. This assessment should take into account that these mortar joints can be considered as planes of weakness, regarding their evolution from the onset of cracking, until failure caused by certain imposed stress states associated with excessive wall/support deformations due to vertical loads.

Considering, essentially, the referred challenges in the study of URM infills cracking due to vertical deflections, the methodology of the present study will consist of the evaluation of buildings with reinforced concrete structures subjected to vertical deformations, based primarily on the analysis of the mechanical characteristics of the URM infill walls. The basic compression behaviour of brick masonry will be assessed, particularly through the previous analysis of a vertical compression test of a masonry specimen, to reveal relevant aspects of the masonry behaviour, when subjected to vertical loads. In particular, the mechanical behaviour characteristics of the constituents (bricks, and mortar joints) will be analysed in order to account for their influence on the compression behaviour of the URM infill.

Based on that evaluation of the mechanical characteristics of the URM infill walls, the analysis of masonry walls subjected to vertical deformations of their supports will be made through the assessment of the relevant characteristic behaviour of masonry wall-beam/slab assembly model, for the case of vertical load. Next, a general modelling approach of the behaviour of URM infills and the interaction with their supports will be accessed, particularly in terms of the analysis of the potential use of numerical methods for the study of that behaviour. It will be specially focused on the correspondent modelling of masonry mortar joints/interfaces mortar joint-brick/mortar joint-concrete beam and the assessment of mechanical characteristics for use in the modelling of URM infill. Lastly, the preventive control of deformations of masonry wall-beam/slab assembly will be discussed, mainly analysing serviceability conditions, which could be impaired by the cracking of infill masonry walls due to excessive vertical deformations of their supporting RC elements.

3 Mechanical Behaviour Characteristics of URM Infills and Their Essential Failures Modes

Combinations of tension, shear, and compression failure modes can be adequately considered through a failure envelope curve for a masonry element, [13], [21], where the tensile failures of the bed joints and cracking of the bricks are included. Detailed modes of failure in a masonry element could be, [28]: cracking of the masonry units in shear; splitting of masonry units in tension; diagonal tension cracking of masonry units; cracking in the joint; sliding along a bed joint. However, tension and shear modes of failure are most common in mortar joints and brick-mortar interfaces, relative to the compression modes of failure.

Numerical analysis is useful for the evaluation of building response under various loading events and, particularly the induced deformations and stresses in infill masonry could be assessed through numerical analysis, as well as to account for the

influence of cracking in the mechanical behaviour of masonry infill and their confining structure elements. For a reliable numerical analysis, it is essential to develop suitable constitutive models related to the masonry units, mortar joints, and masonry units-mortar interfaces, as well as to the interface between the masonry walls and the supporting elements of reinforced concrete.

4 Assessment of Compression Behaviour of Brick Masonry through a Vertical Compression Test of a Masonry Specimen

The interest here is the analysis of the behaviour of infill masonry walls due to the excessive deformation of the reinforced concrete supports when subjected to vertical compression loads, therefore, some relevant features of the masonry behaviour, particularly related to masonry under vertical compression, were previously analysed through a compression test of masonry specimen, described in the following.

4.1 Test Setup

A masonry specimen with two solid clay bricks (Specimen P), linked with a cement mortar joint, was subjected to a compression test (Figure 1), where an increasing vertical load was applied to the specimen until a load of 300 kN was reached, [15]. The two bricks with individual dimensions of 230 mm (length), 70 m m (height), and 110 m m (thickness) had the following relevant characteristics: dry mass of around 2110 kg/m^3; nominal compressive strength of 27.1 MPa; and an estimated value of modulus of elasticity of 8500 MPa. The specimen had a cement mortar (1:1:6 mix by volume of cement, lime, and sand) in the joint (with a thickness near 15 mm) between the first brick (brick in the base of the specimen) and the second brick. A mortar layer (nearly 15 mm in thickness) was laid on top of the second brick to promote, together with cardboard disposed on that layer, a better transmission of the load applied by the loading plate of the compression machine. Therefore, the specimen had, approximately, global dimensions of 230 mm in length, 170 mm in height, and 110 mm in thickness.

Vertical and horizontal displacements in the mortar joint were recorded with four induced transducers (Peekel B60). Absolute vertical (dva1) and horizontal (dha1) displacements were recorded at the central point of the specimen, in the mortar joint (the strains were not recorded in this test; only displacements were recorded). Lateral relative vertical and horizontal displacements at the left side of face A do specimen (respectively, dvr1 and dhr1) and lateral relative vertical and horizontal (respectively, dvr2 and dhr2) displacements, at the respective right side, were measured in the mortar joint, respectively, 37 mm to the left and 37 mm to the right of the central point (Figure 1). Pairs of steel pieces glued in each brick were used for supporting the transducers.

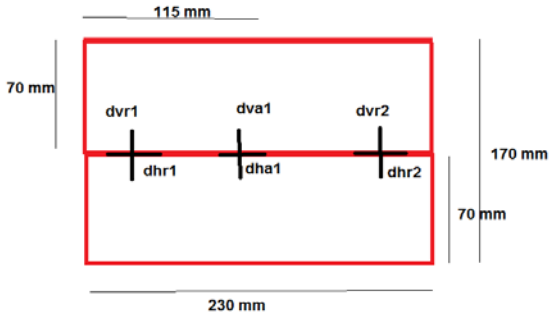

a) Schematic view of Specimen P for the compression test

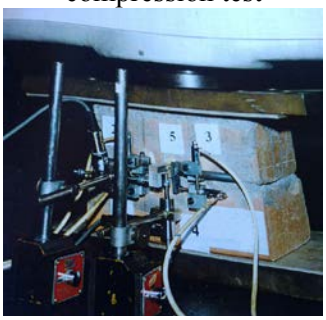

b) Aspect of the instrumentation of the Specimen P for the compression test

Fig. 1: Compression test of Specimen P

The displacements values were registered through data acquisition equipment and the data of the records of six channels, correspondent to the registration of the six displacements above referred, were stored in a file. The load was applied at a constant rate until the maximum load of 300 kN was reached, after which the test was halted and the specimen discharged.

4.2 Test Results

The results of the compression test of Specimen P are presented in Table 2 (Appendix) and Figure 1. These results are, namely related to the measurements of vertical and horizontal displacements in the mortar joint of Specimen P (left lateral relative vertical and horizontal displacements, dvr1 and dhr1) and right lateral

relative vertical and horizontal deformations (dvr2, dhr2)), as referred above in 3.1. In addition, absolute vertical (dva1) and horizontal (dha1) displacements in that mortar joint, at the central point of the specimen, are presented in Table 1 (positive displacements represent a contraction of the transducer spring).

4.3 General Analysis of the Test Results

The test results of Specimen P show, from the start of the test until a value of vertical applied load near 200 kN (8.7 MPa), a variation of relative and absolute vertical displacements (dva1, dvr1, and dvr2) is approximately linear, while the relative horizontal displacements were approximately constant. Thus, these results of the test Specimen P reveal an initial phase of approximate linear behavior in a vertical direction, which was followed, after that level of load of 200 k N, by a phase of test where the non-linear characteristic behaviour of the specimen start to be apparent (Figure 2 and Figure 3).

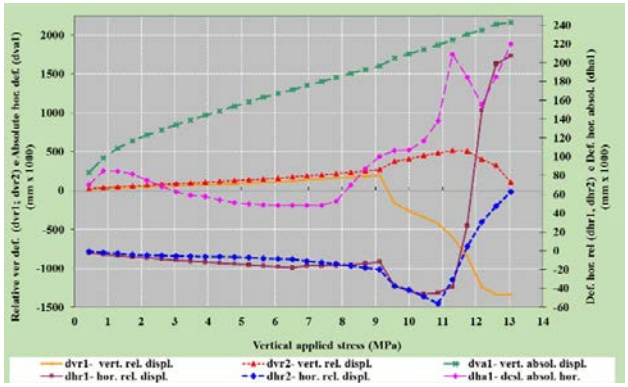

Fig. 2: Results of vertical and horizontal displacements measured in the compression test of the masonry specimen

During the non-linear phase of the test, Specimen P was most likely, in terms of its behaviour, under a complex stress state, and particularly, within the central joint, the state of stress was presumably variable due to the influence of the surrounding two bricks. The test was halted for a maximum load of 300 kN (13.04 MPa), which did not lead to significant cracks and local failure of the specimen. The evident distinct non-linear behaviour, as the load increases from the 200 kN of load towards the maximum load, could be an indication of the micro-cracking of the specimen in that last phase of the test.

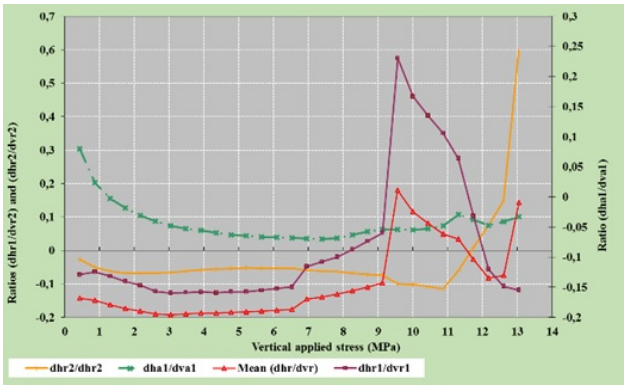

Fig. 3: Ratio between relative horizontal and vertical displacements (dhr1/dvr1 and dhr2/dvr2) and the ratio between absolute horizontal and vertical displacements (dha1/dva1) in the compression test of the masonry specimen

4.3 Influence of the Constituents' Mechanical Characteristics (Bricks, Mortar Joints) on the Behaviour of Specimen P in the Compression Test

The type behaviour of Specimen P during the test is presumed to be significantly influenced by the mechanical characteristics of the constituents (bricks, and mortar joints). As referred above, with the increase of the applied vertical load, during the phase of the test subsequent to a load level of 200 kN, the non-linear behaviour of the specimen was manifest. This non-linear behaviour was most presumably related to the upsurge of micro-cracks due to the significant stress induced in the bricks, and to the substantial differences in elastic properties of units and mortar of specimen P.

These differences are, especially, relevant in this situation of mortar joints considerably softer, when compared with the stiffness of the unit; this type of cement mortar (1:1:6 mix by volume of cement, lime, and sand) is considerably less rigid than the bricks (modulus of elasticity of 8500 M Pa). In this situation, the uniaxial compression of the masonry, in the direction perpendicular to bed joints, can generate a state of triaxial compression in the mortar and a state of compression/biaxial tension in the unit, [9]. The consequent confinement of the mortar joint, imposed by the units, which avoids its lateral expansion, can induce significant stress in the units that potentiate the creation of micro-cracks in the units.

To aid in the analysis of the results of the test of Specimen P, relevant results of previous triaxial tests of mortar of masonry joints and solid bricks, [17], similar to those used in the referred Specimen P, are gathered in the following. The purpose is to enable the suitable interpretation of the results of the

Specimen P test based on the analysis of mechanical characteristics of the constituents (bricks, mortar joints), particularly related to the biaxial compression behaviour of mortar joints and solid bricks.

The referred triaxial compression tests were performed on cylindrical specimens (see the graphic scheme of the specimens in Figure 4), w ith a diameter of approximately 52.5 m m, to which the axial load was applied by means of a hydraulic jack in the triaxial compression machine, and the lateral pressure load was transferred to the specimen fixed inside the triaxial cell. Specimens were made from cement mortar (1:5 mix by volume of cement and sand), and solid bricks similar to the bricks used in Specimen P. The specimens made from solid bricks comprised either specimens without joints or specimens with a single joint. These specimens with a single joint included a diagonal cement mortar joint (1:5 mix by volume of cement and sand), with a thickness of approximately 5 mm, which can be assumed to be in correspondence with the bed joint of Specimen P.

From triaxial compression tests carried out on the referred specimens of mortar and specimens of bricks (without or with mortar joints), which are similar to the cement mortar and bricks used in Specimen P, average stress-strain curves were derived and relevant mechanical properties were estimated, [17].

a) Mortar specimen (MS) b) A brick specimen without joint (SWJ) c) Brick specimen with single joint (SSJ)

Fig. 2: Cylindrical specimens for triaxial tests – mortar specimens and brick specimens

The mortar of the central joint of Specimen P, as exposed before, was presumably, during the test, in a state of triaxial compression, while their two courses of bricks, in certain zones, were likely in a state of compression/biaxial tension. Therefore, the triaxial compression tests of specimens of the mortar are supposed to give valuable information to aid in the analysis of the behaviour of the central joint and the two courses of brick in Specimen P. The specimen made of mortar can give information about the mechanical resistance of the mortar itself in the central joint of Specimen P, while the specimen with a single joint can be useful to help in the analysis of the interface between the bricks and the mortar. The compression triaxial test of specimens of solid brick without joint can provide some indirect indications about the compression/biaxial tension strength of the two courses of brick in Specimen P.

Lateral and axial loads were increased in these triaxial compression tests while maintaining approximately constant chosen values of the respective ratio between lateral compressive stress and vertical compressive stress (σ_L/σ_V) in the specimen until failure was reached. The mentioned chosen values of the ratio of lateral stress/vertical stress, (σ_L/σ_V) in a test of specimens varied between 0.025 and 0.30 (see Table 1): Mortar specimens - σ_L/σ_V = 0.025, 0.05, 0.075, 0.10, 0.2 0, 0.30; Solid bricks specimens - σ_L/σ_V = 0.05, 0.075, 0.10, 0.20, 0.30; Solid bricks specimens with single joint - σ_L/σ_V = 0.05, 0.075, 0.10, 0.20. The type of mortar specimens, solid brick specimens without joints, and solid bricks specimens with single diagonal joint are described in Table 1.

In the specimens of mortar and the specimens with or without joints, vertical displacements could be monitored with a digital transducer, and stress-strain curves (pressure load/vertical displacements) could be obtained.

Additionally, in all those three types of specimens, besides the vertical displacements monitored with a digital transducer, a strain gauge was installed in the face of the specimen, allowing the lateral displacements to be monitored. This strain gauge was placed normally to the vertical axis of mortar specimens or solid brick specimens without a joint and was placed normally to the joint in the specimen with a single diagonal joint. In this case, vertical or lateral pressure versus lateral displacement curves could also be obtained. The relative peak vertical pressure load corresponding to the last load step, before reaching the maximum shear load, was recorded.

The relation of applied vertical load versus vertical or lateral strain for solid brick specimens with a single diagonal joint is presented in Figure 5.

The vertical strains were monitored in all specimens 1c, 2c, 3c, and 4c (negative values correspond to the contraction of the specimens), and lateral strains (positive values correspond to the expansion of the specimens) were monitored only in specimen 4c (with ratio σ_L/σ_V = 0.075)).

Table 1. Type of mortar specimens, solid brick specimens without joint, and solid bricks specimens with single diagonal joint

Type of specimens	**Ratio of lateral stress/vertical stress values (σ_L/σ_V) in test of specimens**		
	Range of ratio of lateral stress/vertical stress values (σ_L/σ_V) in test of specimens	Values of the ratio (σ_L/σ_V) in test of the specimens with recording of vertical strain	Values of the ratio (σ_L/σ_V) in test of the specimens with recording of lateral train and vertical strain
Mortar specimens (MS)	0,025 ≤ σ_L/σ_V≤ 0,30	Specimen 1a = 0.025 Specimen 2a = 0.05 Specimen 3a = 0.10 Specimen 4a = 0.20 Specimen 5a = 0.30	Specimen 6a = 0.075
Solid bricks specimens without joint (SWJ)	0,025 ≤ σ_L/σ_V≤ 0,30	Specimen 1b = 0.05 Specimen 2b = 0.10 Specimen 3b = 0.20 Specimen 4b = 0.30	Specimen 5b = 0.075
Solid bricks specimens with single diagonal joint (SSJ)	0,025 ≤ σ_L/σ_V≤ 0,30	Specimen 1c = 0.05 Specimen 2c = 0.10 Specimen 3c = 0.20	Specimen 4c = 0.075

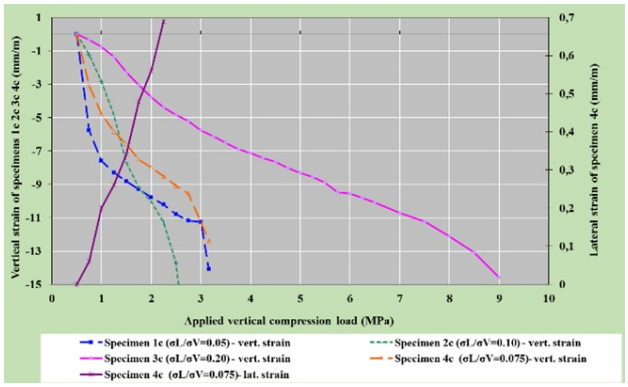

Fig. 3: Vertical stress-vertical or lateral strain relationship for solid bricks specimens with single diagonal joint (SSJ) (lateral and vertical strain were monitored in specimen 4c with ratio σ_L/σ_V = 0.075)

For the particular case of SWJ and SSJ specimens with monitored lateral and vertical strain (ratio σ_L/σ_V = 0.075), the stress/strain relation curves are presented in Figure 6. Figure 6 shows that, with the increase of ratio σ_L/σ_V of the specimens, for values of σ_V less than 1 MPa, the values of the stress/strain relation also increase (denoting that, approximately, the rigidity increases with the increase of ratio σ_L/σ_V, for σ_V less than 1 MPa). It can also be seen that the evolution of the curves of applied vertical stress/vertical or lateral strain relation until σ_V near 1 MPa is approximately linear, and the non-linearity becomes evident after that load, especially for applied vertical stress/vertical strain relation curve.

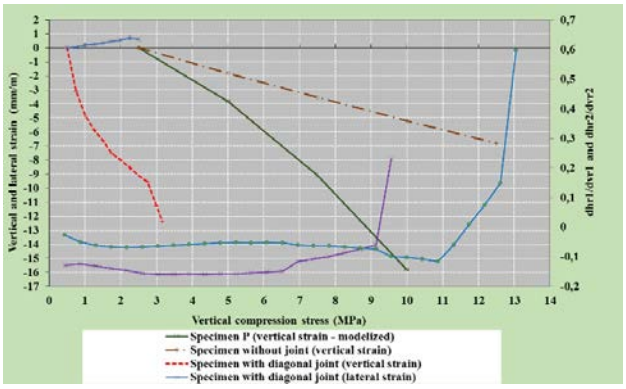

Fig. 4: Stress/strain relationship for solid bricks specimens without joint and specimens with single diagonal joint, corresponding to vertical compression stress-vertical or lateral strain curves (ratio σ_L/σ_V = 0.075)

Figure 7 represents the relationship of peak vertical strain, ε_{max}, with the ratio between peak shear stress and peak vertical stress, τ_{max}/σ_{Vmax}, in the triaxial tests of mortar specimens, solid brick specimens without joint, and solid brick specimens with a single diagonal joint. The mortar specimens are the following: Specimen 1a - σ_L/σ_V=0.025; Specimen 2a - σ_L/σ_V = 0.05; Specimen 3a - σ_L/σ_V=0.10; Specimen 4a - σ_L/σ_V=0.20; and Specimen 5a - σ_L/σ_V = 0.30; Specimen 6a - σ_L/σ_V = 0.075). The solid brick specimens without joint are: Specimen 1b - σ_L/σ_V = 0.05; Specimen 2b - σ_L/σ_V = 0.10; Specimen 3b - σ_L/σ_V = 0.20; Specimen 4b - σ_L/σ_V = 0.30; Specimen 5b - σ_L/σ_V = 0.075). The solid brick specimens with single diagonal joint are: Specimen 1c - σ_L/σ_V = 0.05; Specimen 2c - σ_L/σ_V = 0.10; Specimen 3c - σ_L/σ_V=0.20; Specimen 4c - σ_L/σ_V= 0.075.

The values of relative peak vertical load applied to the specimens correspond to the last registered value (last increment of load) where the ratio of lateral stress/vertical stress, (σ_L/σ_V), during the test, could be kept constant, before the discharge of the specimen occurred. Figure 7 reveals that the vertical strain of MJ specimens is greater than SSJ specimens and SWJ specimens, which means that it could be expected to find the mortar of the central joint of Specimen P, considerably softer than the brick specimen with or without joint in the triaxial test, especially for $\tau_{max}/\sigma_{V,max}$ greater than 0.1. And it reveals also that the vertical strains in the SSJ specimens are greater than the correspondent vertical strains in SWJ specimens, for all $\tau_{max}/\sigma_{V,max}$ values, which can be justified by the presence of a softer mortar joint in SSJ specimens. A parallel

behaviour was observed in the test of Specimen P, with the evident soft behaviour of the central mortar joint linked to the upper and lower bricks considerably more rigid than that mortar joint.

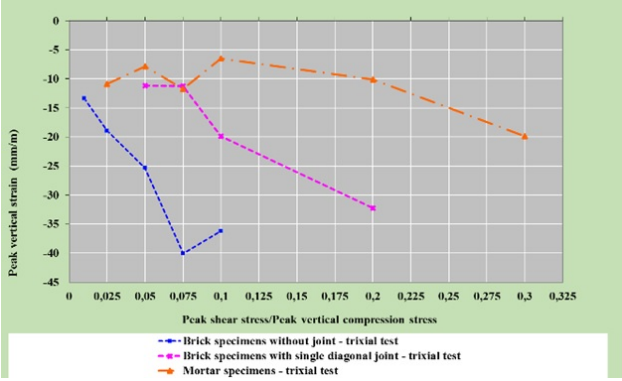

Fig. 5: Peak vertical strain versus the ratio between peak shear stress and peak vertical stress in triaxial tests of mortar specimens (1a - 0.025; 2a - 0.05; 3a - 0.10; 4a - 0.20; and 5a - 0.30; 6a - 0.075), solid brick specimens without joint (1b - 0.05; 2b - 0.10; 3b - 0.20; 4b - 0.30; 5b - 0.075) and solid brick specimens with single diagonal joint (1c - 0.05; 2c - 0.10; 3c - 0.20; 4c - 0.075)

Figure 8, it is presented the relation of applied vertical stress versus vertical and lateral strain (primary vertical axis) in the triaxial test of a specimen with diagonal joint ((SSJ) - σ_L/σ_V=0.075). Also, it is presented in Figure 8 (secondary vertical axis) the ratio between lateral strain and vertical strain of triaxial test of specimens with diagonal joint (dh/dv), and the ratio between horizontal and vertical displacements (dhr1/dvr1 and dhr2/dvr2) in the Specimen P test, for increasing values of applied vertical stress. It can be seen that the triaxial test of specimens with diagonal joint (SSJ), for the particular case of a low ratio of σ_L/σ_V (σ_L/σ_V=0.075), reach a maximum load of three MPa (see Figure 8).

For this range of load (0 to 3 MPa) the values of the ratio between lateral strain and vertical strain of triaxial test of these specimens with diagonal joint (dh/dv) approximately exhibit a similar variation to that of the ratio between horizontal and vertical displacements (dhr1/dvr1) in the Specimen P test. However, in the range of load between 3 MPa and 6 MPa the ratio between horizontal and vertical displacements (dhr1/dvr1 and dhr2/dvr2) of Specimen P remain almost constant.

That behaviour could be a sign that the shear effects in the central joint of Specimen P were, for that range of load of the test (0 to 6 M Pa), still moderate and that the high normal load in the central joint was dominant, compared to the shear stress in that joint. Based on t he variation of dhr1/dvr1 and dhr2/dvr2 in Specimen P (Figure 8), presumably, for stress load greater than 7 MPa, the increase of non-linear behaviour is supposed to have amplified the shear effects in the central joint, although the high normal stress load acting on that joint.

The relation of applied vertical stress versus the ratio between lateral strain and vertical strain (Principal Axis) of triaxial test of specimens without diagonal joint (σ_L/σ_V = 0,075).), is presented in Figure 9. Figure 9, also, is represented the ratio between horizontal and vertical displacements dhr1/dvr1 and dhr2/dvr2 of Specimen P test, for the entire range of the test (Secondary Axis).

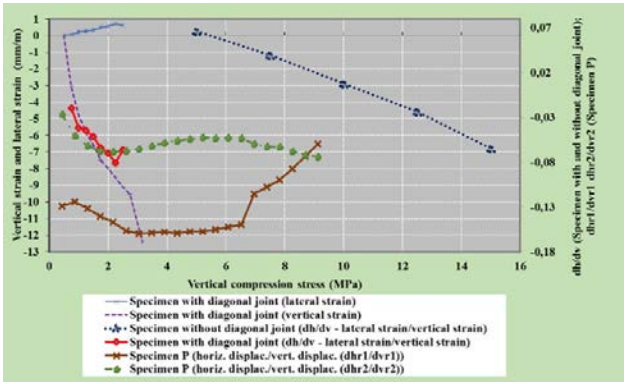

Fig. 6: Variation concerning the applied vertical stress of the vertical and lateral strain of triaxial test of specimens (σ_L/σ_V = 0,075) with diagonal joint (Principal axis); ratio between lateral strain and vertical strain of triaxial test of specimens (σ_L/σ_V = 0,075) with and without diagonal joint (dh/dv) and ratio between horizontal and vertical displacements (dhr1/dvr1 and dhr2/dvr2) of Specimen P test (both ratios in the Secondary axis)

In Figure 10, i t is presented the ratio between lateral strain and vertical strain of the triaxial test of the specimen with diagonal joint ((SSJ) - σ_L/σ_V=0.075), as well as the ratio between horizontal and vertical displacements (dhr1/dvr1) and dhr2/dvr2) of Specimen P test, for increasing values of applied vertical stress.

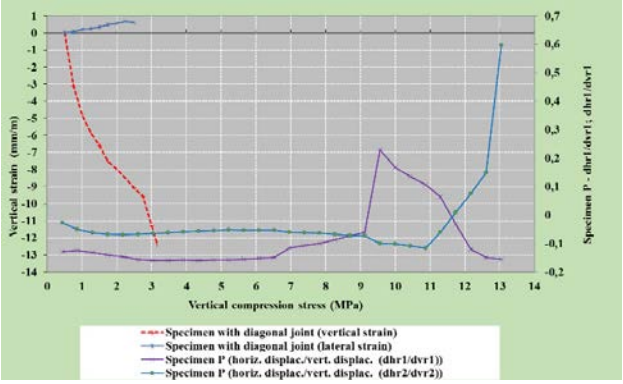

Fig. 7: Relationship of applied vertical stress versus the ratio between lateral strain and vertical strain (Principal Axis) of triaxial test of specimens without diagonal joint (σ_L/σ_V = 0,075); Ratio between horizontal and vertical displacements dhr1/dvr1 and dhr2/dvr2 of Specimen P test (Secondary Axis)

It can be seen that the triaxial test of specimens with diagonal joint (SSJ), for the particular case of a low ratio of σ_L/σ_V (σ_L/σ_V=0.075), ended near a load of 3 MPa (see Figure 9). However, for this range of load (0 to 3 MPa) the values of the ratio between horizontal and vertical displacements (dhr1/dvr1 and dhr2/dvr2) of Specimen P are almost constant. That could be a sign that the shear effects in the central joint of Specimen P were still moderate, for that range of load of the test (0 to 3 MPa), and that the high normal load in the central joint was dominant compared to the shear stress in that joint.

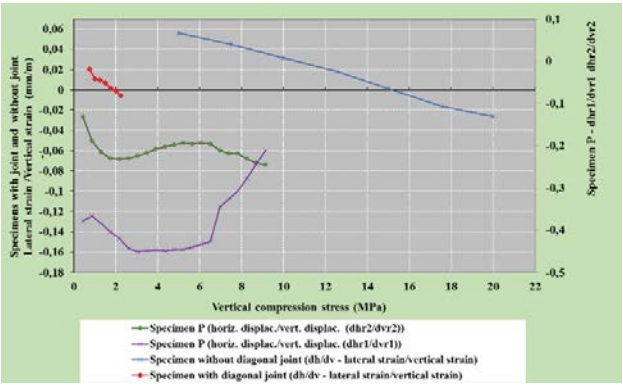

Fig. 8: Relationship of applied vertical stress versus the ratio between lateral strain and vertical strain (Principal Axis) of triaxial test of specimens with and without diagonal joint (σ_L/σ_V = 0,075); Ratio between horizontal and vertical displacements dhr1/dvr1 and dhr2/dvr2 of Specimen P test (Secondary Axis)

Based on the variation of dhr1/dvr1 and dhr2/dvr2, in Figure 9, presumably, for stress load greater than 7 MPa, the increase of non-linear behaviour is supposed to have increased the shear effects in the central joint, even though the high normal stress load present.

5 Characteristic Behaviour of Masonry Wall-Beam/Slab Assembly in Case of Vertical Deformations

The vertical deformations of masonry walls supporting RC elements can cause appreciable cracking of these masonry walls, which requires that the basic behaviour of masonry wall-beam/slab assembly should adequately be accessed.

5.1 Basic Behaviour of Masonry Wall-Beam/Slab Assembly

For the particular case of a masonry wall made of bricks and mortar joints similar to that analysed in chapter 3, a practical option is to analyse the masonry wall-slab/beam assemble behaviour related to vertical deformations, through an idealised model of a masonry wall-beam assembly, simply supported, subjected to a uniformly distributed vertical load at the top of the wall. In this model, both vertical stresses and shear stresses at the wall-beam interface are concentrated towards the supports, [8], [16], with symmetrical distribution (Figure 11), eventually leading to arching action (formation of an arching thrust). These vertical and shear stresses can have a maximum value at each end part of the beam and gradually decrease their value, approximately, to zero, at a distance to the half span that will depend, in great part, on the flexibility of the beam.

The above referred idealised model of a masonry wall-beam assembly allows us to estimate the vertical and shear stress distribution at the wall-beam interface, [8], [19]. Based on numerical simulation by the finite element method, [8], it was shown that, for wall-beam assembly, the distribution of stresses at the interface of the wall with the beam (vertical pressure exerted by the wall on the beam) could be considered approximately linear, parabolic or cubic type, respectively for values of a stiffness parameter K_d greater than 7, between 7 and 5, and lesser than 5, being K_d defined by:

$$K_d = \left[\frac{E_w . t . h^3}{E_b . I_b}\right]^{\frac{1}{4}} \quad (1)$$

E_w - elastic modulus of the masonry wall;
E_b - elastic modulus of the beam;
t, h - width, and height of the masonry wall;
I_b - moment of inertia of the section of the beam.

The maximum vertical stress in the masonry wall (peak compression value at the supports that increases with the increase of K_d; see f_m in Figure 11) is given by:

$$f_m = \left[\frac{W_w \,.\, C_1}{\mathrm{l}\,.\,\mathrm{t}}\right] = p_w \,.\, C_1 \qquad (2)$$

l - span of the beam;
W_w - total vertical load in the beam/wall assembly;
p_w - mean pressure vertical load in the wall;

The maximum shear stress along the interface wall/beam is given by:

$$\tau_m = \left[\frac{W_w . C_1 . C_2}{l . \mathrm{t}}\right] \qquad (3)$$

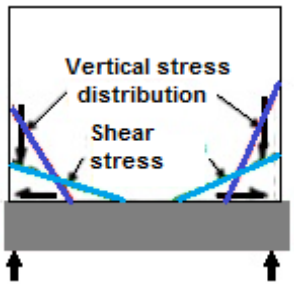

Fig. 9: Model of wall-beam assembly with vertical and shear forces in beam, [8]

Considering the results of numerical simulation by finite element method, these values of vertical and shear stresses are defined in relation to the parameters C_1 and C_2, being C_1 the value of vertical stress concentration in the wall above referred, [8]. These parameters are related to K_d and to the constants α, ß, e γ (see definition of these constants in Figure 12).

$$C_1 = 1 + \beta . K_d \qquad (4)$$

$$C_2 = \alpha + \Upsilon . K_a \qquad (5)$$

Where K_a is defined as follows:

$$K_a = \left[\frac{E_w . t . h}{E_b . A_b}\right] \qquad (6)$$

A_v – Area of the beam cross-section (A_b = B.d; B, d – respectively, width and height of the beam)

K_a can also be expressed as in the following, considering the above definition of K_d

$$K_a = 12 . (K_d)^4 . \left[\frac{h}{d}\right]^2 \qquad (7)$$

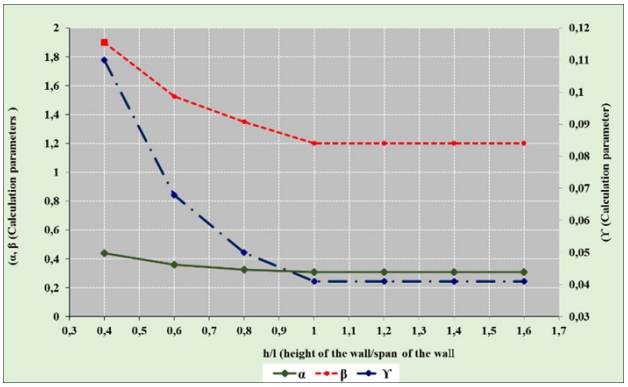

Fig. 10: Definition of the constants α, ß, e γ, [8]

5.1 Shear and Compressive Stresses in Masonry Wall-Beam/Slab Assembly

The ratio between maximum shear stress along the interface wall/beam (τ_m) and maximum vertical stress (compression) in the masonry wall (f_m) is given by:

$$\frac{\tau_m}{f_m} = \left[\frac{1}{C_2}\right] = \left[\frac{1}{\alpha + \Upsilon . K_a}\right] \qquad (8)$$

Changing the previous equation to include the stiffness parameter K_d instead of K_a, the ratio τ_m / f_m can be expressed as follows:

$$\frac{\tau_m}{f_m} == \left[\frac{1}{\alpha + 12 . \Upsilon . (K_d)^4 . \left[\frac{h}{d}\right]^2}\right] \qquad (9)$$

The relation between the ratio peak shear stress/peak vertical compression stress (τ_m/f_m) and the peak vertical strain in the triaxial tests referred in the previous section 4 (specimens with or without joint and mortar specimens) is presented in Figure 13. It is also presented, Figure 13, the relation between that ratio (τ_m/f_m) and the value of stiffness parameter K_d of a wall-beam/slab assembly. From Figure 13, it can be shown that, with the increase of the ratio τ_m/f_m and consequently of the shear action in the interface wall/beam, the value of stiffness parameter K_d decreases, reducing the concentration of compressive stress near the supports.

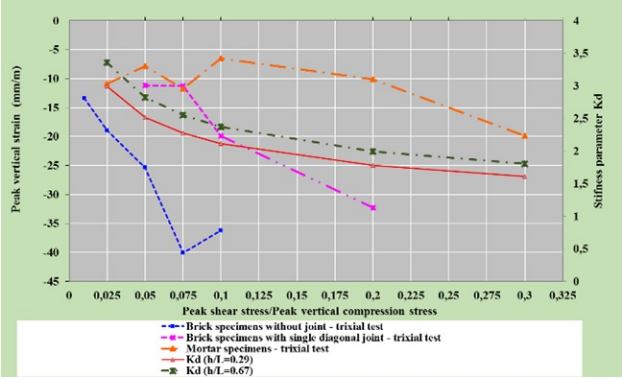

Fig. 11: Relationship of the Ratio between Peak shear stress/Peak vertical compression stress (τ_m/f_m) versus vertical strain of triaxial test of specimens with or without joint and mortar specimens; and relationship of the Ratio τ_m/f_m versus the value of stiffness parameter K_d

It can be found a similar tendency of variation of the stiffness parameter K_d and the peak vertical strain, and that, with the increase of the ratio τ_m/f_m (more pronounced shear effects when compared with the effect of vertical compression stress), possibly, the vertical strain could be further increased, either in the mortar joints or in the bricks itself, while, as referred before, the concentration of compressive stress near the supports is lowered due to the reduction of K_d.

The evolution of vertical strain of bricks and mortar joints, for high values of ratio τ_m/f_m, when their internal cracking could be progressing until the end of the test (Figure 13 – near the end of the triaxial tests), allows us to suppose that the mechanical properties of the URM infill (in-wall/beam assemble) can be significantly changed after the cracking of the mortar joints and brick-mortar interfaces and with the possible decrease of masonry stiffness and increase of non-linear behaviour (K_d also has, for these high values of ratio τ_m/f_m, a decreasing tendency). These deductions can be eventually supported by the detected variation, described before, of dhr1/dvr1 and dhr2/dvr2 in Specimen P (Figure 8), which indicates that, presumably, for high-stress loads, the increase of non-linear behaviour is supposed to have amplified the shear effects in the central joint, although the high normal stress load acting on that joint.

6 General Modelling Approach of Masonry Walls Behaviour

Numerical models are useful for the evaluation of building response under various loading events, particularly to account for the influence of cracking on the mechanical behaviour of masonry infill and their confining RC elements.

6.1 General Modelling Approach

The URM infill response to the normal actions, particularly the vertical loads acting in the wall/beam assemble is significantly dependent on the complex behaviour at a micro level, such as stress redistribution among constituents, damaged induced anisotropy, or strain localisation.

Numerical methods allow the comprehension and prediction of the behaviour of URM infill up to its failure and collapse, particularly in the case of the vertical loads acting in the wall/beam-lintel assemble, [20], [26], [30]. A detailed analysis of the induced deformations and stresses on those masonry walls subjected to vertical deformations of their supports could be carried out through numerical analysis.

The numerical analysis of URM infills requires the implementation of an adequate computational strategy that takes into account the complex behaviour of URM infill. That numerical analysis can be based, particularly, on macro-models that assume masonry material as a fictitious homogeneous continuum; micro/meso-modelling, which considers the micro-structure, including the interaction between the masonry constituents; and multi-scale modelling based on h omogenisation techniques.

Macro-models can be suitable in certain cases of numerical analysis of large URM infills, owing to their limited computational cost, [24]. Particularly, some types of macro-models applied to masonry consider this material as a fictitious homogeneous orthotropic continuum, with no di stinction between units and joints in the discrete model, an assumption that can present some difficulties with the mechanical parameters of the continuum to be used and with the definition of the failure criteria. In the situation of wall-beam assemble where the strain localisations can occur in the masonry micro-structure near the supports (high compression zone), that probably could lead to a type of dissipation mechanism that requires to be adequately considered the influence, on the macroscopic properties, of the changing of the micro-structure.

The micro/meso-modelling could be suitable to be used in the case of detailed modelling of the total micro-structure of URM infills with limited dimensions, [11], [12], [25], allowing to consider the interaction between the masonry constituents, although involving a complex model generation, which must be limited, in case o f wall/beam

assemble, to small masonry elements, in order to avoid high computational costs.

Certain options of modelling mortar joints can possibly minimise these computational costs such as, [27]: model mortar joints and mortar-brick interface by the zero-thickness element, although this assumption implies that brick-mortar interaction is not considered; no distinction to be made between the failure of the brick-mortar interface and mortar layer; and tensile splitting of the brick units under compression to be not considered, which is probably acceptable only if crushing zone near the supports of the wall-beam assemble the bricks were far from a tensile splitting failure.

Computational homogenisation techniques can be regarded as being between macro and micro modelling techniques, and possibly could be a possible option for the research analysis of the wall/beam assemble with large dimensions subjected to vertical loading, since, in this case of multi-scale modelling based on homogenisation techniques, detailed and time-consuming modelling of the total micro-structure of URM infills could be avoided; the macro-structure scale is assumed as an equivalent homogeneous medium and the behaviour of the heterogeneous micro-structure is considered by solving a micro-scale problem on a representative sample of the micro-structure, [14], [29], [1]. This type of multi-scale modelling has to deal with difficulties related to the occurrence of strain localisation in the micro-structure.

In multi-scale approach, the mesoscopic and macroscopic scales of representation are intrinsically coupled. Some type of multi-scale approaches bridges both scales, by the identification of macroscopically used material parameters from mesoscopic models and the structural computation is then performed with the macroscopic model only, [1]. In this approach, closed-form constitutive relations need to be postulated for both scales and it was used particularly, for modelling the elastic behaviour of masonry.

Several multi-scale models were proposed, in the following, are referred some relevant examples: an enhanced multi-scale model using non-local implicit gradient isotropic damage models for both the constituents, describing the damage preferential orientations and employing, at the macroscopic scale, an embedded band model, [14], micro-mechanical model for masonry homogenisation in the nonlinear domain, incorporating suitably chosen deformation mechanisms coupled with damage and plasticity models, [29], multi-scale approach for the analysis of the in-plane masonry response, adopting a Cosserat model at the macro-level and a classical Cauchy medium at the micro-structural, [1].

6.2 Modelling of Masonry Mortar Joints and the Interfaces Mortar Joint-Brick and Mortar Joint-Concrete Beam

Cracking in URM infills may be located at brick-mortar interfaces, mortar joints, or in both of the referred zones.

Numerical analysis intended to account for the influence, in the URM infill mechanical behaviour, of their cracking due to vertical deformations of the supporting RC elements, should be based on an adequate evaluation of mechanical behaviour characteristics of the URM infill. That evaluation of mechanical behaviour characteristics allows the subsequent development of adequate constitutive models relative to the masonry units, mortar joints, and masonry units-mortar interfaces, as well as to the interface between masonry and the supporting RC elements of the infill masonry walls. These constitutive models could be implemented in numerical models of the finite element method for the analysis of URM infill walls subjected to vertical deformations of their supports.

Among relevant approaches used to model the cracking of mortar joints, it can be highlighted the "Smeared crack approach" and the "Discrete crack approach". The "Smeared crack approach" is suitably used for cases where the cracking of masonry is modelled within a continuum medium, but in this approach, the numerical solution is dependent on the mesh size, and there could be some difficulties in fully capturing diagonal shear cracks in failure of mortar and brick, particularly in the specific case of the top part (corner zones) of wall/beam assemble, where these shear cracks are possible.

A discrete crack approach could be adequate for modelling cracks in quasi-brittle materials such as masonry, which is based on the theory of fracture mechanics and fictitious crack model, and although in this approach it is generally necessary to change finite element mesh at each crack increment, there is a correspondent low mesh sensitivity benefit.

The onset and spread of cracking of URM infill walls due to the excessive deformations of the RC supports can lead to a significant change in the mechanical behaviour of these walls, and a progressive decrease of their mechanical strength with the increasing deformations of the referred supports. Particularly, the onset of cracking in masonry walls depends on masonry mortar joints (bed joints and head joints), which influence,

decisively, their post-cracking behaviour and consequently their failure mode. That change of masonry mechanical behaviour related to cracking and to the eventual non-linearity, inherent to the advanced phase of the cracking process, is admitted to be reliably assessed through numerical analysis.

Adequate numerical models should be able to analyse the relation between excessive vertical deformations of the supporting RC element of masonry walls and the consequent anomalies particularly related to the cracking of masonry walls.

Particularly, the cracking modelling approach should capture the specific patterns of cracking in the masonry walls due to excessive deformations of their supports. Furthermore, the consideration of the referred nonlinear behaviour of masonry walls in the numerical analysis strongly depends on the type of modelling approach and correspondent constitutive models of masonry elements implemented in the numerical tools.

6.3 Basic Mechanical Characteristics for Use in the Modelling of URM Infill

Some basic mechanical parameters of masonry are essential to develop constitutive models such as modulus of elasticity, E, shear modulus, G, and Poisson´s ratio.

As an example of accessing these mechanical parameters of masonry, in following is considered the specific case of brick masonry analysed before (in chapter 2), where, in particular, it is possible the evaluation of uniaxial compressive stress-strain relationship based on the compression test of Specimen P, to obtain some of these relevant mechanical parameters and of significant characteristics of the mechanical behaviour of masonry under axial compression.

The uniaxial compression test of the specimen P was not conducted until the collapse of the specimen but was ended for a stress load of 13.04 MPa (axial load of 300 kN) which was greater than a stress load that can be considered yield stress of the compression test. Analysing the results (Figure 2 and Figure 3) it is possible to identify the yield stress of the specimen between 8 MPa and 9 MPa, and it can be fixed, as the conventional value of yield stress, load stress of 8.5 MPa. To evaluate a possible uniaxial compressive stress-strain relationship of the test, it was taken the value of the characteristic compressive strength of the masonry, f_k, as an approximation of the yield stress value. According to Eurocode 6 (EN 1996-1-1: 2005, 3.6.1.2 - equation 3.2, [6], (for masonry made with general purpose mortar and lightweight mortar)), f_k (in N/mm^2) can be assumed as:

$$f_k = f_b^{\,0.7} \cdot f_m^{\,0.3} \tag{10}$$

Where:

f_k is the characteristic compressive strength of the masonry, in N/mm^2;

K is a constant and, where relevant, modified according to 3.6.1.2(3), [6];

f_b is the normalised mean compressive strength of the units, in the direction of the applied action effect, in N/mm^2;

f_m is the compressive strength of the mortar, in N/mm^2

Although the strains were not recorded, as referred above, in this test, the applied stress during the uniaxial compression of masonry, f_{mu}, can, approximately, be related to peak stress f_{max} (f_{max} is denoted as f , in Figure 14) and to the peak strain ε_{ml}, [7], as follow:

$$f_{mu} = \left[\frac{2.\varepsilon}{\varepsilon_{ml}} - \left(\frac{\varepsilon}{\varepsilon_{ml}}\right)^2\right] . f_{max} \tag{11}$$

Therefore, the applied stress in the uniaxial compression of masonry, f_{mu}, can be related to peak stress, f_{max} (considering that $f_k \approx f_{max}$), the peak strain ε_{ml} and the compressive strength of block and mortar, i.e., f_b (brick) and f_m (mortar), as follow:

$$f_{mu} = \left[\frac{2.\varepsilon}{\varepsilon_{ml}} - \left(\frac{\varepsilon}{\varepsilon_{ml}}\right)^2\right] . f_b^{\,0.7} . f_m^{\,0.3} \tag{12}$$

In the present case, f_b (normalised mean compressive strength of the units) is near 27.1 MPa and f_m (compressive strength of the mortar) is near 2.7 MPa, [17]. Assuming a value of peak strain ε_{ml} near 12 mm/m (it appears acceptable considering the peak strain of the triaxial test of a specimen with joints (σ_L/σ_V=0.075 – Figure 7), results in the following expression:

$$f_{mu} = \left[\frac{2.\varepsilon}{\varepsilon_{ml}} - \left(\frac{\varepsilon}{\varepsilon_{ml}}\right)^2\right] . f_b^{\,0.7} . f_m^{\,0.3} \tag{13}$$

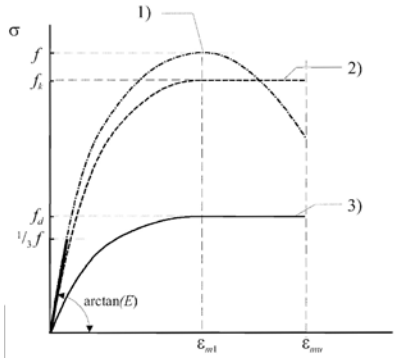

1) typical;
2) idealised diagram (parabolic-rectangular)
3) design diagram
ϵ_{ml} – strain of masonry for peak load;
ϵ_{mu} - limiting compressive strain in masonry

Fig. 12: Stress-strain relationship for masonry in compression (EC6, 2005, [6])

Figure 15 presents the modelled vertical strain of Specimen P (uniaxial compressive stress-vertical strain relationship of Specimen P test, according to equation (13)) and the ratio between horizontal and vertical displacements dhr1/dvr1 and dhr2/dvr2 of Specimen P test, for the entire range of the test (both denoted in the Secondary Axis).

The eventual micro crack formation due to vertical compressive stress of a masonry specimen leads to the increase of the volume of the material, which is commonly designated as dilatancy. The ratio between the normal and shear displacements is denoted as the tangent to the dilatancy angle (tan ψ). Experimental results, [2], [28], [18], revealed that dilatancy is, essentially, a function of tangential relative displacement and normal stress. Generally, the reduction of dilatancy angle is associated both with the increase of relative tangential displacement, due to the loss of cohesion in joints of brick-mortar interface and with the progressive smoothing of asperities of the joints, under the action of increasing normal stresses.

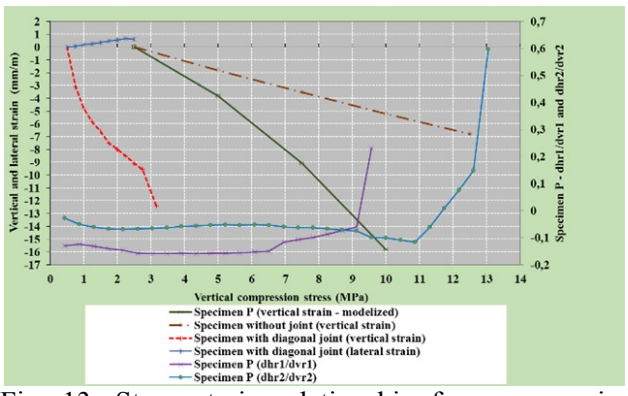

Fig. 13: Stress-strain relationship for masonry in compression (triaxial tests of specimens and compression test of Specimen P)

In Figure 15, it is represented (in the Principal vertical axis) the variation, with the vertical applied stress load, of the estimated modulus of elasticity of the specimen without joint and of the mortar specimen in the triaxial tests (σ_L/σ_V = 0,075 - instantaneous value computed dividing the increment of vertical displacements of specimens between consecutive load steps). Relatively to Specimen P, it is represented, in Figure 15 (in the Principal vertical axis), the values of a vertical deformation coefficient (in MPa), which was computed by dividing the increment, between consecutive load steps, of vertical absolute displacements in the compression test of specimen P, by the half height of the Specimen (h=170 mm). This coefficient has a certain analogy to a modulus of elasticity. In addition, it is presented, in Figure 15 (in the Secondary vertical axis), the values of a coefficient associated with dilatancy in the compression test of specimen P, which was computed through the calculation of the ratio between horizontal and vertical displacements dhr1/dvr1 and dhr2/dvr2 in the Specimen P test. This coefficient has a certain analogy to the tangent to the dilatancy angle (tan ψ).

About the evaluation of deformation characteristics of the type of masonry of Specimen P, the short-term secant modulus of elasticity of masonry, E (Young's modulus - Figure 14), in the absence of a value determined by tests in accordance with EN 1052-1, may be taken as dependent of f_k, as recommended in Eurocode 6 (EN 1996-1-1 :2005, 3.7.2, [6]: $E = K_E \cdot f_k$, and the recommended value of K_E is 1000). According to Eurocode 6 (3.6.1.2 - equation 3.3), f_k can be expressed in terms of normalised mean compressive strength of a masonry unit, f_b for masonry made with thin layer mortar, in bed joints of thickness 0,5 mm to 3 mm, and clay units of Group 1 (EN 1996-1-1:2005, 3.1.1 (Types and grouping of masonry units), [6]: Tab.3.1, [6] - Group 1:Volume of holes (% of gross volume) ≤ 25), being K=0.75 (Tab.3.3, [6]) - f_b = 27.1 MPa):

$$f_k = K.f_b^{0.85} = 0.75x27.1^{0.85} = 12.4 \text{ MPa} \quad (14)$$

Therefore, the modulus of elasticity (Young's modulus), for the type of masonry of Specimen P, is obtained, as follows:

$$E = K_E f_k = 1000x12.4 = 12.4 \text{ GPa} \quad (15)$$

Other relevant parameters related to the type of masonry of Specimen P are shear modulus, G, initial shear strength, f_{vko}, (estimation under zero compressive stress) of the bricks, and initial interface cohesion of mortar joint (estimation under zero compressive stress), friction angle ϕ (friction coefficient, $\mu=\tan\phi$) and Poisson's ratio, ν. of the bricks. The shear modulus, G, may be taken as 40 % of the modulus of elasticity, E (EN 1996-1-1:2005, 3.7.3, Shear modulus (1), [6]), thus the shear modulus, G, for the type of masonry of Specimen P, can have estimated a value of 5 GPa. Based on the triaxial tests referred to before, [17]) the estimated values for the following parameters are presented in the following: initial shear strength of the bricks – 4.09 MPa; initial interface cohesion of mortar joint – 0.36 MPa; friction angle ϕ (friction coefficient, μ) of the bricks - 54º (degrees); friction angle ϕ of the mortar joints - 39º (degrees) and Poisson's ratio, ν, for bricks - 0.17.

7 Preventive Control of Deformations of Masonry Wall-Beam/Slab Assembly

Along the service life of the buildings with reinforced concrete structure, their serviceability conditions can be impaired by the cracking of infill masonry walls, which are related, generally, to their brittle behaviour and low tensile strength, [22], [19].

Excessive vertical deformations of masonry walls supporting RC elements can lead, in certain cases, to deficiencies of aspects of these supports (sharp curvature of the beams and slabs) and, more often, to the cracking of the masonry walls, [23]. Moreover, these vertical deformations, possibly, could affect the out-of-plane (OOP) capacity of URM infills related to wind action, since their influence on the OOP bearing capacity of the boundary conditions could be relevant, particularly in terms of appreciable detrimental effects in the resistance of the connections of the URM infills at their top and/or at their bottom, due to the time-dependent deflections of their supporting RC elements.

Several experimental studies were made aiming at the assessment of limiting values for the deflections of RC supporting elements corresponding to initial visible cracks, [3], [23], [20]. And, in the case of masonry walls cracking associated with the deformation of the supporting elements, the deflection at the mid-span, corresponding to the onset of visible cracking in the masonry wall (in certain cases a horizontal crack in the base of the wall), is generally low, less than about 1/2000 of the span, [4], [3], [23].

Thus, it is essential the careful monitoring of the problems related to building serviceability associated with masonry cracking due to excessive deformations of the supports of the URM infill walls, through an adequate survey of the problems and analytical studies, namely based on numerical analysis of the URM infill walls and their RC supporting elements.

These analytical studies should take into account that, besides the cases where deformations of an RC support should not exceed certain limiting value that adversely affects its proper functioning or appearance, these deformations should not exceed those that can be accommodated by other connected elements such as partitions, glazing, cladding, services or finishes. Particularly the application of numerical analysis to the study of these problems should aim to verify that, according to EC6 (see EN 1996-1-1:2005 - Section 7, Serviceability Limit State,7.1 General, [6]), the serviceability of masonry members should not be impaired by the behaviour of other structural elements, such as deformations of floors or walls.

Generally, the serviceability limit states in buildings should take into account, particularly, stiffness criteria expressed in terms of limits for vertical deflections. Deflections and limiting values may be obtained from ISO 4356 Norm (ISO 4356, 1977, [10]. The appearance and functionality of the structure could be reduced when the sag of the support (beam/slab) subjected to quasi-permanent loads exceeds span/250 (see EC2 - EN 1992-1-1:2004, [5]).

8 Conclusion

The mechanical characteristics of the URM infill walls as well as of their interface with the supporting concrete elements were here analysed, aiming at the evaluation of buildings with reinforced concrete structures subjected to vertical deformations. The basic compression behaviour of brick masonry was assessed, particularly through the previous analysis of a vertical compression test of a masonry specimen, which revealed relevant aspects of the masonry behaviour when subjected to vertical loads.

The behaviour of Specimen P during the test was found to be significantly influenced by the mechanical characteristics of their constituents (bricks, and mortar joints). With the increase of the applied vertical load, the non-linear behaviour of the

specimen was manifest. This non-linear behaviour was most presumably related to the upsurge of micro-cracks due to the significant stress induced in the bricks, and to the substantial differences in elastic properties of units and mortar of specimen P.

The mechanical behaviour characteristics of the constituents (bricks, and mortar joints) was analysed in order to account for their influence in the compression behaviour of the URM infill, aiming particularly for the prevision of their cracking in case vertical deformations of the supporting RC elements. Based on that evaluation, the analysis of masonry walls subjected to vertical deformations of their supports was made through the assessment of the relevant characteristic behaviour of the masonry wall-beam/slab assembly model, for the case of vertical load. It could be presumed, from that analysis, that the evolution of a vertical strain of bricks and mortar joints for high values of ratio τ_m/f_m, when their cracking could be progressing, allows supposing that the mechanical properties of the URM infill (in-wall/beam assemble) can be significantly changed after the cracking of the mortar joints and brick-mortar interfaces and with the possible decrease of masonry stiffness and increase of non-linear behaviour.

Thus, an approach for modelling mortar cracking should be required in order to improve a suitable numerical model for mortar joints and brick-mortar interfaces. For that evaluation, it is essential to develop suitable constitutive models of the masonry units, mortar joints, and masonry units-mortar interfaces, as well as of the interface between masonry and the supporting RC elements. The potential application of the main types of numerical analyses, in the study of buildings based on reinforced concrete structures subjected to vertical deformations, is considered to be reliably accessed.

A comprehensive analysis of the mechanical characteristics of the URM infill walls and of the behaviour of masonry wall-beam/slab assembly is considered to have been suitably made in this paper, with positive repercussions in terms of their better knowledge, in view of possible further development of a detailed analysis specifically using numerical methods. Hence, it is admitted that the present paper can provide, for future scientific research work, a helpful reference for the evaluation of URM infills subjected to excessive deformations of their supports, considering the contribution of the paper for revealing essential features of the masonry behaviour under vertical compression and for highlighting relevant characteristics of the behaviour of masonry wall-beam/slab assembly subjected to vertical loads, as well as the correspondent risk of URM infill cracking due to excessive deformations of the RC elements.

As possible future developments of this work, it is recommendable that should be further studied, deeply, the use, in the analysis of the behaviour of the wall-beam/slab assemble under vertical load, of macro-models, micro/meso-modelling and multi-scale modelling based on homogenisation techniques, with the corresponding evaluation of the advantages and disadvantages of each of the above-referred modelling techniques; and that should also be studied, extensively, the mechanical behaviour characteristics of the URM infill, aiming the subsequent development of the respective constitutive models for their implementation in numerical analysis.

References:

[1] Addessi, D., Elio Sacco A multi-scale enriched model for the analysis of masonry panels International Journal of Solids and Structures, 49, 2012, pp. 865–880.

[2] Atkinson R., H., Amadei B. P., Saeb S., Response of masonry bed joints in shear. J. Struct. Eng. Proc. ASCE, 115:9, 1989, pp. 2276–96.

[3] Burhouse, P., Composite action between brick panel walls and their supporting beams. Building Research Station. BRS CP2/70, 1969, Watford, Herts.

[4] *(text in French)* Centre Scientifique et Technique de la Construction, CSTC. La fissuration des maçonneries. Bruxelles, CSTC, Note d´information technique 65, 1967.

[5] EN 1992-1-1. Eurocode 2: Design of concrete structures - Part 1-1: General rules and rules for buildings. Brussels: CEN, 2004.

[6] EN 1996-1-1. Eurocode 6: Design of masonry structures - Part 1-1: General rules for reinforced and unreinforced masonry structures. Brussels: CEN, 2005.

[7] Hemant B.K., Rai D.C., Jain S.K., Stress-strain characteristics of clay brick masonry under uniaxial compression. Journal of Materials in Civil Engineering; 19, 2007, pp. 728-39.

[8] Hendry A, W., Masonry Walls in Composite Action. Structural Masonry, 1998.

[9] Hilsdorf, H. K. - An investigation into the failure mechanism of brick masonry loaded in axial compression. Designing, engineering and constructing with masonry products, ed. F. B.

Jonhson, Gulf, Houston, Texas, 1969, pp. 34-41.

[10] *(text in French)* ISO 4356, Bases du calcul des constructions – Déformations des bâtiments à l´état limite d´utilisation. Genève: ISO, 1977.

[11] Lotfi H.R., Shing P.B., Interface model applied to fracture of masonry structures. J. Struct. Eng. 120:1(63), 1994. https://doi.org/10.1061/(ASCE)0733-9445,

[12] Lourenço, P.B., Rots J.G., Multisurface interface model for analysis of masonry structures. J. Eng. Mech., 1997. https://doi.org/10.1061/(ASCE)0733-9399(1997) 123:7(660).

[13] Mann W.; Müller H., Failure of shear-stressed masonry - An enlarged theory, tests and application to shear walls. Proceedings of the British Ceramic Society, 1982, pp. 223-35.

[14] Massart, T.J., Peerlings, R.H.J., Geers, M.G.D., An enhanced multi-scale approach for masonry wall computations with localization of damage. International Journal for Numerical Methods in Engineering, 69(5), 2007, pp. 1022-1059.

[15] *(text in Portugese)* Miranda Dias J. L., Composite action between lightweight concrete masonry blocks and their supporting beams (in Portuguese). Ph.D. Thesis, IST, LNEC, Lisboa, 1997.

[16] Miranda Dias, J. L., Cracking around the interface joint between masonry panels and their supporting reinforced concrete beams in buildings. Proceedings of 2nd International Structural Engineering and Construction Conference, vol. I, University of Rome, Italy, 2003, pp. 745–52. https://scholar.google.com/scholar?oi=bibs&cluster=10607007199108459364&btnI=1&hl=pt-PT

[17] Miranda Dias, J. L., Susceptibility for cracking of masonry mortar joints when subjected to compression. Proceedings of 10th Canadian Masonry symposium, University of Calgary, Alberta, Canada, S. 3b; 2005. https://scholar.google.com/scholar?oi=bibs&cluster=4992547139043150709&btnI=1&hl=pt-PT

[18] Miranda Dias, J. L. Cracking due to shear in masonry mortar joints and around the interface between masonry walls and reinforced concrete beams. J. Constr. Build. Mater., 21, 2007, pp. 446–457. https://doi.org/10.1016/j.conbuildmat.2005.07.016.

[19] Miranda Dias, J. L., Assessment of anomalies related to vertical deformations in heritage buildings with reinforced concrete structure and infill masonry walls. Congresso "Reabilitar & Betão Estrutural 2020 – Reabilitar & BE2020". Lisboa, LNEC, 2021, pp. 789-801. https://scholar.google.com/scholar?oi=bibs&cluster=14780750394293614 86&btnI=1&hl=pt-PT

[20] Page, A. W., Non-linear analysis of composite action of the masonry walls on beams. Proc. Instn. Civil Engrs, Vol. 2, 67, Mars 1979, pp. 93-110.

[21] Page, A.W., The strength of brick masonry under biaxial tension-compression. Int. Journal Masonry Construction, 3(1), 1983, pp. 26-31.

[22] Page, A. W., The serviceability design of low-rise masonry structures. Prog. Struct. Eng. Mater, Vol.3, Issue 3, 2001, pp. 257-267.

[23] *(text in French)* Pfefferman, O., Fissuration des cloisons en maçonnerie due à une déformation excessive du support. Étude experimentale. CSTC - Revue, Bruxelles, 4, 1975.

[24] Roca, P., Cervera, M. , Pelà, L., Clemente, R., Chiumenti, M., Viscoelasticity and damage model for creep behaviour of historical masonry structures. Open Civ Eng J, 6, 2012, pp. 188–199.

[25] Sacco E, Toti J. Interface elements for the analysis of masonry structures. Int. J. Comput. Meth. Eng. Sci. Mech., 11(6), 2010, pp. 354-373. https://doi.org/10.1080/15502287.2010.516793

[26] Stavroulaki, Maria E., Liarakos, Vagelis B., Dynamic analysis of a masonry wall with reinforced concrete lintels or tie-beams. Engineering Structures 44, 2012, pp. 23-33. http://dx.doi.org/10.1016/j.engstruct.2012.05.041

[27] Stavridis, A., Shing, P. B., Finite-element modeling of nonlinear behaviour of masonry infilled RC frames. J Struct Eng, 11, 2010, pp. 354-373. https://doi.org/10.1038/342131c0.

[28] Van der Pluijm, R., Rutten, H., Ceelen, M., Shear behaviour of bed joints. 12th international brick/block masonry conference, 2000. doi: 10.1111/j.1743-6109.2012.02948.x.

[29] Zucchini, A., Lourenço, P. B., A micro-mechanical homogenisation model for masonry: Application to shear walls. International Journal of Solids and Structures, 46 (3-4), 2009, pp. 871-886,.

[30] Mazur, W., Drobiec, L., Jasinski, R., 2017, Research and numerical investigation of masonry – AAC precast lintels interact. International Conference on Analytical Models and New Concepts in Concrete and Masonry Structures AMCM'2017. Procedia Engineering 193, 2017, pp. 385-392.

Contribution of Individual Authors to the Creation of a Scientific Article (Ghostwriting Policy)

José Dias had the ideas and was responsible for formulation of overarching research goals and aims of this paper. Also, José Dias was responsible for conducting the research and for the development of the methodology of the study. Moreover, José Dias has organized the experiments referred in the section 4, and was responsible for their execution. Lastly, José Dias carried out the preparation, creation of the published work.

Sources of Funding for Research Presented in a Scientific Article or Scientific Article Itself

The Planned Research Programme of the "National Laboratory of Civil Engineering" (LNEC) has funded the present study.

Conflict of Interest

The author has no conflict of interest to declare that is relevant to the content of this article.

APPENDIX

Table 2. Results of the compression test of Specimen P

Axial load			Displacements					
kN	**MPa**	**% Max. Load**	**dhr1**	**dvr1**	**dhr2**	**dvr2**	**dha1**	**dva1**
10	0.43	0.03	-2.29	17.71	-0.5	18.71	70.17	230.83
20	0.87	0.07	-3.86	31	-1.79	35.5	84.92	420.08
30	1.3	0.1	-5.14	39.07	-2.93	47.64	84.75	546.67
40	1.74	0.13	-6.36	45.29	-3.93	58.29	81.5	639.42
50	2.17	0.17	-7.43	50.64	-4.64	67.86	74.83	714.17
60	2.61	0.2	-8.71	55.64	-5.21	77.21	68.17	781.67
70	3.04	0.23	-9.86	61.79	-5.64	86.79	62.75	846.42
80	3.48	0.27	-10.93	68.86	-6	96.79	59.17	909.25
90	3.91	0.3	-11.86	75.07	-6.21	106.5	57.67	968.67
100	4.35	0.33	-12.93	81.29	-6.5	116.29	54.08	1026.33
110	4.78	0.37	-13.93	88.43	-6.86	127.07	51.17	1087.5
120	5.22	0.4	-15.07	95.64	-7.21	137.57	49.67	1142.92
130	5.65	0.43	-16.07	103.64	-7.93	149.14	48.83	1197.5
140	6.09	0.47	-17	111.57	-8.43	160.36	48.67	1246.25
150	6.52	0.5	-18	120.43	-9.14	171.93	48.67	1295.25
160	6.96	0.53	-15.86	137.43	-11.21	187.64	48.58	1355.17
170	7.39	0.57	-15.93	148.14	-12.5	200.21	48.58	1401.33
180	7.83	0.6	-15.79	158.5	-13.57	215.14	52.92	1451.58
190	8.26	0.63	-14.79	169.5	-15.93	234.64	69.42	1507.92
200	8.7	0.67	-13.43	182.29	-18.21	252.64	87.33	1556.08
210	9.13	0.7	-11.71	196.14	-20	269.93	100.42	1603.58
220	9.57	0.73	-37.21	-161.5	-37.36	374.29	106.5	1702.75
230	10	0.77	-42.79	-256.21	-41.57	409.64	106.83	1755.92
240	10.43	0.8	-45.86	-339.36	-48.5	449.43	117.08	1813.5
250	10.87	0.83	-44.71	-421.57	-55.93	484.71	138.08	1871.5
260	11.3	0.87	-38.36	-599.71	-31.07	512.14	208.58	1937
270	11.74	0.9	26.64	-847.79	4.5	509.64	184.83	2011.83
280	12.17	0.93	149.43	-1242.43	30.57	403.64	155.25	2062.92
290	12.61	0.97	198.57	-1336.07	47.64	320.93	185	2138
300	13.04	1	207.14	-1338	62.43	18.71	219.58	230.83